Available online at www.sciencedirect.com
ScienceDirect
International Journal of Machine Tools & Manufacture 47 (2007) 1164–1175
INTERNATIONAL JOURNAL OF MACHINE TOOLS & MANUFACTURE DESIGN, RESEARCH AND APPLICATION
www.elsevier.com/locate/ijmactool

Role of mandrel in NC precision bending process of thin-walled tube

Li Heng, Yang He*, Zhan Mei, Sun Zhichao, Gu Ruijie

Department of Materials Forming and Control Engineering, College of Materials Science and Engineering, Northwestern Polytechnical University, P.O. Box 542, Xi'an 710072, PR China

Received 25 May 2006; received in revised form 29 August 2006; accepted 1 September 2006
Available online 8 January 2007

Abstract

The thin-walled tube NC bending process is a much complex physical process with multi-factors coupling interactive effects. The mandrel is the key to improve bending limit and to achieve high quality. In this study, one analytical model of the mandrel (including mandrel shank and balls) has been established and some reference formulas have been deduced in order to select the mandrel parameters preliminarily, i.e. mandrel diameter d, mandrel extension e, number of balls n, thickness of balls k, space length between balls p and nose radius r. The experiment has been carried out to verify the analytical model. Based on the above analysis, a 3D elastic–plastic FEM model of the NC bending process is established using the dynamic explicit FEM code ABAQUS/Explicit. Thus, the influences of mandrel on stress distribution during the bending process have been investigated, and then the role of the mandrel in the NC precision bending process such as wrinkling prevention has been revealed. The results show the following: (1) Wrinkling in the tube NC bending process is conditional on membrane biaxial compressive stress state; the smaller the difference between the biaxial membrane stresses is, the more possibility of wrinkling occurs. (2) If the mandrels of larger sizes are used, it will cause the neutral axial to move outward and the difference between the in-plane compressive stresses to become more obvious, which may increase minimum wrinkling energy and anti-wrinkling ability. But the larger mandrel sizes make outside tube over-thinning. (3) When the mandrel extension length increases, the neutral axial will move outward and the difference between the biaxial compressive stresses becomes larger, but the significance is less than that of the mandrel diameter. The excessive extension will cause tube to over thin or even crack. (4) The significance of ball number's effect on the neutral axial position and difference between biaxial compressive stresses is between ones of mandrel diameter and mandrel extension. Increasing the ball number will enhance the thinning degree and manufacturing cost. The results may help to better understanding of mandrel role on the improvement of forming limit and forming quality in the process.

Keywords: Thin-walled tube; NC bending; Mandrel; Wrinkling; ABAQUS/explicit

1. Introduction

The NC bending process of thin-walled tube has been attracting more and more applications in aerospace, aviation, automobile and various other high technology industries, due to its high forming precision advantage and satisfying the increasing needs for high strength/weight ratio products. The technology has become one of frontier fields in the research and development of advanced plastic forming technology [1].

The rotary-draw-bending method is commonly employed in the thin-walled tube NC bending process. The key technique to realize precision and stable bending deformation is how to select the optimal parameters and control the stress and strain states reasonably. Thus, the degrees of ovalization and thinning of bent tube can be controlled to some acceptable extent under free wrinkling conditions.

In order to reduce the wrinkling risk and cross-section distortion degree, it is considered to fill the thin-walled tubes with fine sand or rosin-cerate. Also, the larger tube bending operations are often filled with sand to prevent wrinkling. But it is known that filling the mediums such as sands or fluid may decrease the forming precision in practice and add fore-treatment and post-treatment processes such as sealing, removing sealing and materials cleaning; thus, increasing forming cost and environmental

*Corresponding author. Tel.: +86 29 8849 5632; fax: +86 29 8849 5632.
E-mail address: yanghe@nwpu.edu.cn (Y. He).

0890-6955/$ - see front matter © 2006 Elsevier Ltd. All rights reserved.
doi:10.1016/j.ijmachtools.2006.09.001

pollution, etc., which seems difficult to satisfy the requirements of advanced NC bending process. While the mandrels can overcome the above problems due to its advantages of designability, much flexibility and relative little cost. The mandrel is of importance to improving both the forming limit and the bending quality. So the research on the role of the mandrel is of great significance in the thin-walled tube bending process.

Many scholars have carried out the researches on the tube bending process using FEM. But most of them focused on the stretch bending, the press bending, the pure bending or the hot bending. Up to now, study on the thin-walled tube NC bending process, especially the influence of the mandrel on the process is still scant [2–6]. In the authors' lab, the wrinkling phenomena in the thin-walled tube bending process were investigated by importing the proposed wrinkling predictor into the self-development rigid–plastic FEM code TBS-3D [7–10]. However, due to the complication of the physical process with tri-linearity and multi-factors coupling interactive effects, it is difficult to realize the simulation in the rigid–plastic FE simulation modeling in correlation with the true dynamic contacts conditions between tube and various dies such as tube between mandrel and balls.

Consequently in the study, to carry out the study on the mandrel role in the advanced bending process, based on the analytical description of the mandrel in the thin-walled tube bending process, a 3D elastic–plastic FEM model of the process is established for the process, then the mandrel's (including mandrel shank and balls) influence on stress distribution have been investigated and thus the mandrel role in the bending process has been discussed.

2. Analytical modeling of mandrel in NC bending

2.1. Experimental method

In the thin-walled tube NC bending process, as shown in Fig. 1, both sides of the tube are subjected to various tooling's strictly contacting force, such as bend die, clamp die, pressure die (with or without boost device), wiper die and mandrel (with one or more flexible balls). The tube is clamped against the bend die; Drawn by the bend die and the clamp die, the tube goes past the tangent point and rotates along the groove of the bend die to the desired bending degree and the bending radius. Thus, the bending deformation is finished and then the mandrel is withdrawn and the tube is unloaded. So the process needs precise coordination of various dies and strictly controlling of forming parameters.

Among the above toolings, the ball-and-socket-type flexible mandrel (including balls) is positioned inside the hollow tube to provide the rigid support. The mandrel is composed of mandrel shank and balls. As shown in Fig. 1, the mandrel can be precisely described by the mandrel diameter d, the mandrel extension length e, the number of balls n, the thickness of balls k, the space length between balls p and the nose radius r. Among them, the mandrel extension e refers to the mandrel shank extension length exceeding the point of tangency.

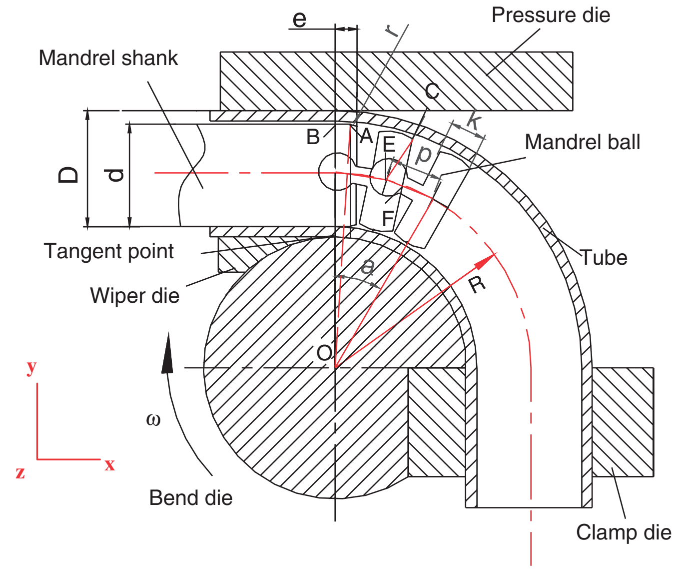

Fig. 1. Forming principle of Rotary draw bending method and sketch of standard mandrel.

2.2. Analytical modeling of the mandrel

According to the plastic forming features in the tube bending process and the geometry cooperation of mandrel/tube, the reference formulas are deduced in order to select the above mandrel parameters faster and preliminarily. The assumptions and basic theory used are as follows:

(1) In the tube bending process, the connection between the mandrel shank and the balls satisfies the "natural connection" principle-namely ideal contact condition meaning there is no interference between each other.
(2) In the bending process, the balls rotate about Z-axis and should point to the bending center O due to the requirements of achieving steady metal materials deforming and increasing the balls service life shown in Fig. 1.
(3) The tube undergoes the bending deformation from the early stable stage to stable one, and only the materials in the local regions near the tangent line deform largely and the possible wrinkling, over-thinning and severe section ovalization may occur in this regions.

As shown in Fig. 1, in the right-angled triangle Rt OAB, the value of AB can be calculated by Eq. (1):

$$AB = \sqrt{(R + D/2 - t)^2 - (R + d/2)^2} \quad (1)$$

where the nose radius r plays the function of the smooth transition.

Then the maximum extension length $e_{\max}$ can be obtained by Eq. (2):

$$e_{\max} = \sqrt{(R + D/2 - t)^2 - (R + d/2)^2} + r \quad (2)$$

From the above formula, it is shown that the mandrel extension length largely depends on the relative tube diameter D/t, the bending radius R and the mandrel diameter d. When the mandrel extension length exceeds the maximum length $e_{\max}$, the tube will interfere with the mandrel shank and over thins or then cracks. It is noted that the minimum extension length $e_{\min}$ should equal r. If the mandrel extension length is less than r, the mandrel and wiper die would not cooperate well and the wrinkling may happen.

The thickness of balls k should be reasonable. The excessive thin k can not ensure the mechanical connection strength. Whereas when the k is too thick, the clearance between tube and point C on balls is too big to exert the rigid support services. Here, is one coordination formula of the k based on the geometry cooperation:

$$D/2 - t - \sqrt{(d/2)^2 - (k/2)^2} < c_{\max} \tag{3}$$

where $c_{\max}$ is the maximum value of clearance, $\sqrt{(d/2)^2 - (k/2)^2}$ is the value of AF in the right-angled triangle Rt CEF.

When the cross-section degree with maximum ovalization is α, the effective arc α_e is as below:

$$\alpha_e = \alpha - \operatorname{arctg}\frac{e}{R - D/2 + t} \tag{4}$$

where $\operatorname{arctg}(e/(R - D/2 + t))$ is the radian corresponding to the mandrel extension length.

Then the number of flexible balls can be calculated by

$$n = \frac{R - D/2 + t}{k}\alpha_e \tag{5}$$

The space length between balls p is obtained according to the geometry relationship as shown in Fig. 1 when n and k are given:

$$p = R \times \alpha/n \tag{6}$$

2.3. Modeling validation

In order to verify the above proposed analytical modeling of mandrel, the experiment has been carried out.

The experimental parameters are the follows: tube outside diameter D is 38 mm, wall thickness t 1 mm. The bending radius R 57 mm, R/D 1.5. The mandrel diameter 35.60 mm, the nose radius r 6 mm. Additionally, according to the experimental results and tube bending characteristics, the cross-section degree α with maximum cross-section ovalization equals about $\pi/4$ rad for the bending angle $\pi/2$ rad.

According to the above formulas, the mandrel parameters can be calculated under the above mentioned experimental bending conditions. The maximum extension length $e_{\max}$ is 11.5 mm, the number of balls n 2, balls thickness $k_{\max}$ 12 mm, the space length p between mandrel shank and balls 15 mm.

The results show that if the mandrel parameters are selected within the above calculated ranges, the preliminary tolling setup is carried out well. With no more than three times trials, the bending operations are accomplished with free-winkling and both section ovalization and thinning degrees are welled controlled.

Table 1
Mandrel extension length for different dies

Specification	Mandrel diameter d (mm)	Maximum extension length $e_{\max}$ (mm)
∅38 × 1 × 38	35.6	10.7
∅38 × 1 × 42	35.6	10.9
∅38 × 1 × 57	35.6	11.5
∅50 × 1 × 60	47.6	11.8
∅50 × 1 × 75	47.6	12.3

Table 2
Mandrel balls parameters

Specification	Balls thickness k (mm)	Space length between balls, p (mm)	Number of balls, n
∅38 × 1	12.00	15.00	2
∅50 × 1	20.00	25.00	2

Thus the rationality of the above formulas is validated. Additionally, the mandrel extension length and the reference values for mandrel parameters for the other 4 kinds tube bends are also obtained as Tables 1 and 2. The formulas may amend the previous empirical formulation and help to better understanding and fast selection of the mandrel parameters in the FE simulation modeling and practical situation.

3. FEM modeling and key problems resolved

Compared with the static implicit algorithm, dynamic explicit FE algorithm is the main method for simulation of the metal forming process with unique advantages such as little solution costs, few difficulties in simulating complex contact and large deformation process, also ability of predicting wrinkling and cross-section distortion phenomena directly, without iteration or convergence tolerance. So based on the prior research [8–10] and according to the practical tube bending process, a 3D elastic–plastic FE model of the NC bending process is established using the FE code ABAQUS/Explicit (shown in Fig. 2).

To model the quasi-static metal forming process using explicit algorithm exactly, some control parameters such as mass scaling factor and speed scaling factor need to be considered carefully, also the key problems such as element type, friction condition, materials properties and contact condition are selected reasonably [11].

3.1. Geometry modeling and assembling

The NC bending process requires the precise coordination of the five parts such as bend die, clamp die, pressure

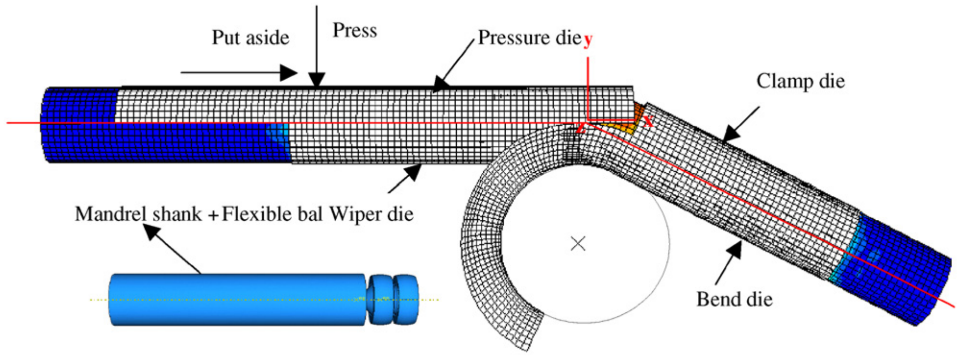

Fig. 2. Illustration of FEM model for NC bending process.

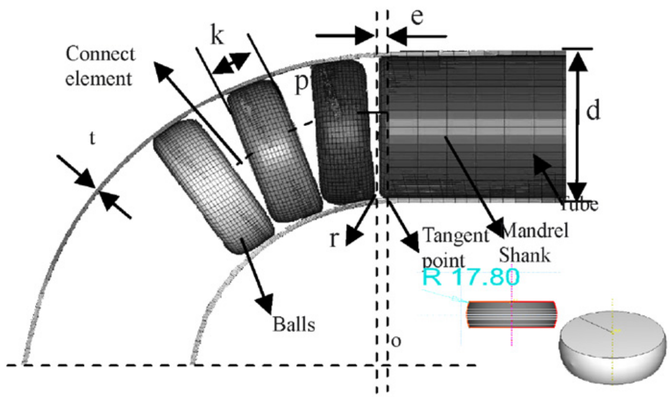

Fig. 3. Geometry model of mandrel with three balls.

die (assistant push), wiper die, and mandrel with one or more flexible balls. Balls rotate depending on the tube bending operations. Fig. 3 shows the geometry model of mandrel shank and flexible balls with the same contact mechanism as practice by defining the identical dynamic attributes to the real contact conditions.

3.2. Element-type selection and materials properties

The four-node doubly curved thin shell S4R is adapted to describe three-dimensional deformable tube with the following features: reduced integration and hourglass control. Five integration points are selected across the thickness to describe the tube bending deformation better. The tube is divided into two parts axially: a clamped portion and a to be bent portion. The clamped portion of the tube is held between the bend die and the clamp die during the bending process. The to be bent portion will actually undergo the bending deformation. The total number of meshing elements is 5889. The external and internal rigid tools are modeled as rigid bodies using 4-node 3-D bilinear quadrilateral rigid element R3D4 to describe smooth contact geometry curved faces.

Correct material properties determine the credibility of the FE simulation. The uniaxial tension test is used to

Table 3
Mechanical properties of tube

Materials	1Cr18Ni9Ti	LF2M
Ultimate tension strength σ_b (MPa)	680	190
Extensibility δ (%)	53	22
Poisson's ratio, γ	0.28	0.34
Initial yield stress, σ_s (MPa)	357	90
Hardening exponent, n	0.373	0.262
Strength coefficient K	1422	398
Young's modulus E (GPa)	169	56
Density ρ (kg/m^3)	7800	2700

obtain the mechanical properties of stainless steel (1Cr18Ni9Ti) and aluminum alloy (LF2 M) as shown in Table 3. And the material model is the commonly used Swift's power-law plastic model as in Eq. (7):

$$\bar{\sigma} = K\bar{\varepsilon}^n \tag{7}$$

3.3. Friction formulation

In the tube bending process, five contact interfaces between tube and dies are as following: tube/mandrel (ball), tube/wiper die, tube/bend die, tube/clamp die and tube/pressure die. Because the plastic deformation zone only concentrates on local small areas, and most of tube parts still belong to non-deformation zone, namely rigid zone, the classical Coulomb model has been chosen to represent the interfaces' friction conditions:

$$\sigma_f = \mu|\sigma_n| \tag{8}$$

where σ_f is the frictional stress, μ the friction coefficient ($0<\mu<0.5$), σ_n the stress on the contact surface.

The tube's bending deformation depends on the contact and friction between various tube portions and different dies. According to the different contact conditions, the friction coefficient can be classified into 4 kinds: 0.05, 0.1, 0.25 and "Rough", in which "Rough" type refers to no relative slipping when nodes contact each other and suitable for the tube/clamp die friction conditions. And the different friction coefficients have been assigned to the different contact interfaces as shown in Table 4.

3.4. Dynamic boundary conditions

The contact interfaces between the tube and the dies are defined with the "Surface-to-surface contact" option, which allows sliding between these surfaces. And the "Kinematic constraints" is used to describe the mechanical constraints combined with "Penalty method" to improve the computation efficiency and accuracy. Moreover, according to the real conditions, the sliding formulation for every contact interfaces is the "Finite sliding" except the one for tube/clamp die contact pair with the "Small sliding", namely not being allowed for sliding between the contact surface.

The "Displacement/rotates" and "Velocity/angular" are used to apply the same boundary constraints and loadings as the true bending process. For the bending process with the bending radius 57 mm, the bending time needed is 1.96 s at the bending speed 0.8 rad/s.

Both bend die and clamp die are constrained to rotate about the global Z-axis, while the pressure die is constrained to translate only along the global X-axis with the same linear speed as the centerline bending speed of the bend die. The wiper die is constrained along all the degrees of freedom. And the trapezoidal profile is used to define the smooth angular velocity of the bend die, the clamp die and the pressure die.

The mandrel's speed along X-axis is 0 in the bending process. After the bending operation is finished, the mandrel will be withdrawn. The relative movement between mandrel shank and flexible balls is complex. The "Connector element" is employed to define the contact conditions between mandrel shank and floating balls. The translating and rotation degrees of freedom are all 0 except that the rotation degree of freedom about Z-axis is free.

3.5. Model validation by experiments

The established elastic–plastic FE model is verified by using PLC controlled bender W27YPC-63NC with the same forming principle and dies structure as the NC bending machine.

Table 4
Friction conditions in various contact interfaces

	Contact interface	Friction coefficients
1	Tube/wiper die	0.05
2	Tube/pressure die	0.25
3	Tube/clamp die	Rough
4	Tube/bend die	0.1
5	Tube/mandrel	0.1
6	Tube/balls	0.1

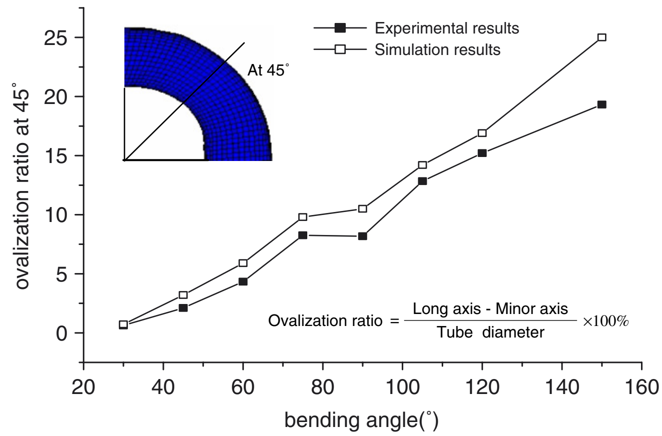

Fig. 4. Comparison of simulation result with Experiment: (a) mandrel diameter 34.2 mm; (b) mandrel diameter 35 mm; and (c) mandrel diameter 35.6 mm.

The experimental conditions: the material is aluminum alloy (LF2 M). The tube outside diameter D 38 mm, the thickness t 1 mm, the bending radius R 57 mm, the bending angle is 90°. The bending speed is 0.15 rad/s, the pressure die's assistant pushing speed is 8.55 mm/s. The mandrel length is 153 mm, the pressure die length is 250 mm, the clamp die length is 115 mm, and the wiper die length is 120 mm. The lubricant is stainless steel oil extrusion S980B. The mandrel diameter is 35.60 mm, the extension length e is 6 mm, the balls thickness k is 12 mm, the number of balls n is 1, the space length between balls p is 15 mm and the nose radius r is 6 mm.

It is experimentally found that the cross-section distortion degree of the mid-cross-section is almost maximum among the distortion degrees of tube cross-sections and the cross-section distortion is one of the deformation phenomena of the bent tube. So the cross-section distortion degree at 45° is used to verify the FE modeling with the bending angle 90° in the study.

Fig. 4 shows the comparison of FE cross-section distortion degrees with experimental ones. It is found obviously that the maximum distortion degree increases linearly when the bending angle rises and the calculation error between the simulation and the experimental results is less than 5%. So the tube can be bent stably on the above conditions. Thus the model is validated.

4. Results and discussion

Using the established explicit FE model, the influence mechanism of the mandrel on the complex stress distribution has been revealed, and then the role of the mandrel in the NC bending process has been revealed.

The simulation condition: the mandrel diameter is 34.2, 35.0 and 35.6 mm, respectively. According to Eq. (1), the corresponding maximum mandrel extension length e_{max} is 16.9, 14.6 and 11.47 mm. Thus, the mandrel extension length is selected as 6, 8, 10 and 11 mm, and the number of balls is 0, 1, 2 and 3. Other parameters are the same as the ones in the above experiment.

4.1. Effects of mandrel diameter size

The FE calculation of the bending processes with the mandrels of different sizes 34.2, 35.0 and 35.6 mm have been carried out, respectively. The mandrel extension length e is 6 mm and the ball number is 2. When the mandrel diameters are 34.2 and 35.0 mm, the wrinkling occurs for both aluminum alloy and stainless steel tubes; while there are free wrinkles when the mandrel diameter is 35.6 mm. The maximum tangent stress distributions for the mandrels of different sizes have been investigated. Fig. 5 shows the history curves of maximum tangent stresses with various mandrels of different sizes.

It is found that the tube's maximum tangent compressive stress is greater than maximum tension stress all over the stable bending process with the maximum difference from 10% to 12% when the size of the mandrel diameter is small; however, when the mandrel diameter is 35.6 mm, the maximum tangent compressive stress is nearly the same as the maximum tension stress, even smaller than the tension stress in some moments. So the larger mandrel size can enable both the tangent compressive and tension stresses to become close mostly. And according to the "Moment Balance" principle, the maximum tangent compressive stress approaching tension stress represents that the neutral axis extends toward outside tube from inside, which increases the minimum wrinkling energy and thus anti-wrinkling ability.

Fig. 6 shows that though the wrinkling occurs with the mandrel size 34.2 and 35.0 mm, the corresponding maximum tangent compressive stresses are less than the one with the mandrel size 35.6 mm. Thus, it is unreasonable to predict the wrinkling only according to the value of the tangent compressive stress. Unfortunately, the compressive stress has been used as the wrinkling prediction criterion in most previous literatures. It is found that wrinkling in the tube NC bending process is conditional on membrane biaxial compressive stress state in the process. So the

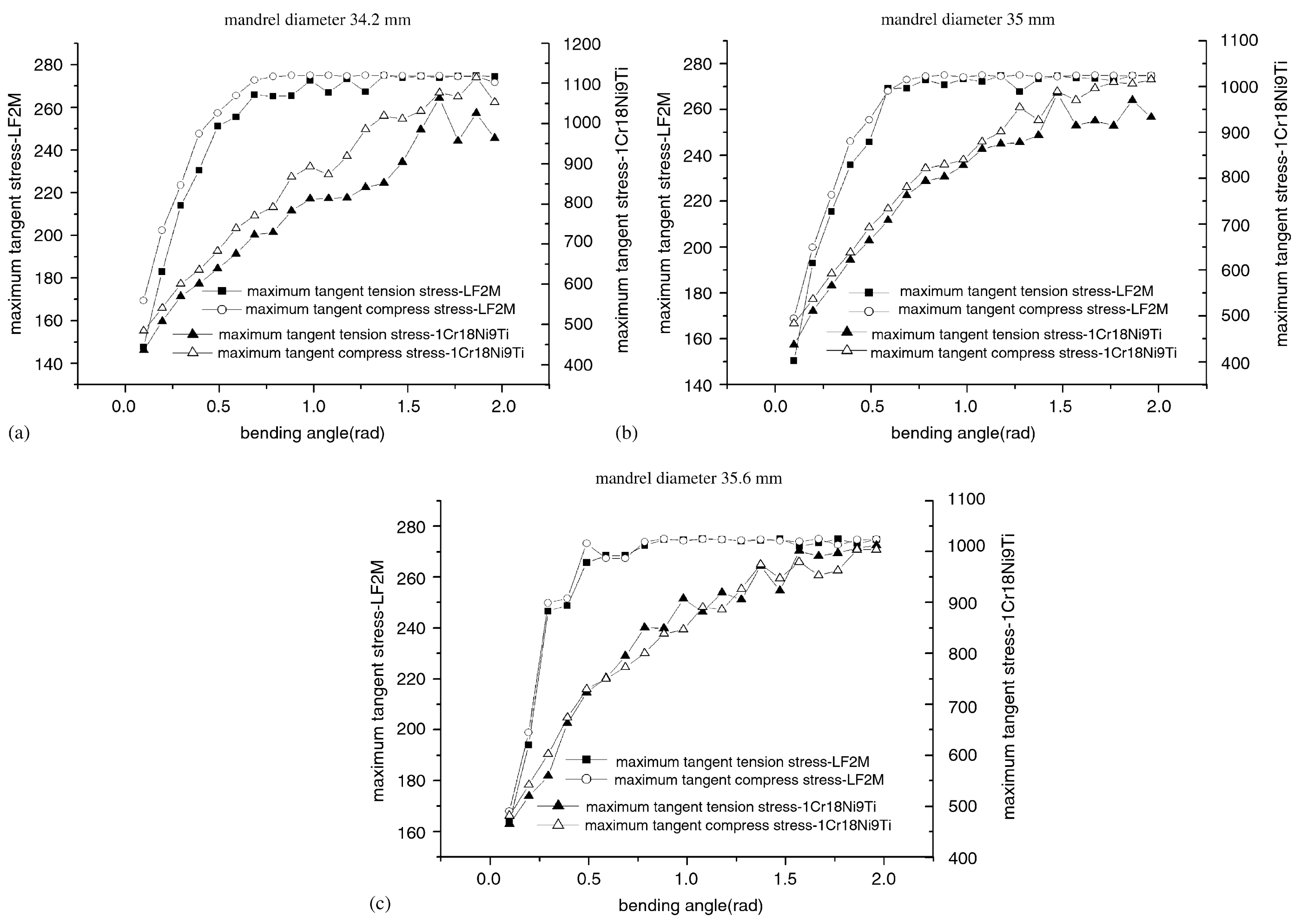

Fig. 5. History curve of maximum tangent stress with different mandrel diameters ($e = 6$ mm, $n = 2$): (a) mandrel diameter 34.2 mm; (b) mandrel diameter 35 mm; and (c) mandrel diameter 35.6 mm.

comparison between the tangent compressive stress and the circumferential stress in the stable period is carried out.

Fig. 7 reveals that the difference between the maximum tangent and circumferential compressive stress becomes more obvious with the larger mandrel size. Just as founded that when the mandrels of the larger sizes are used, the wrinkling tendency may become littler. Namely, the larger the difference between the in-plane biaxial compressive stresses is, the less possibility of wrinkling occurs.

But it is noted that, with too large mandrel size, the extrados thinning degree may become larger and larger, or even crack. Sometimes, there'll exist a risk that the relative slipping between tube and clamp die will happen due to the large drag force exerted by the friction between tube and mandrel, which may cause the wrinkles.

So the maximum mandrel diameter $d_{\max}$ should be optimized based on the minimum mandrel diameter $d_{\min}$ for free winkling. The minimum mandrel diameter $d_{\min}$ can be calculated by Eq. (9):

$$d_{\min} = D - 2t - 2c_{\max} \tag{9}$$

In the study, the maximum clearance $c_{\max}$ for free wrinkling between the tube and the mandrel is 0.2 mm for the bent tube with 38 mm outer diameter and 1 mm thickness. Thus the mandrel diameter is 35.6 mm by Eq. (9).

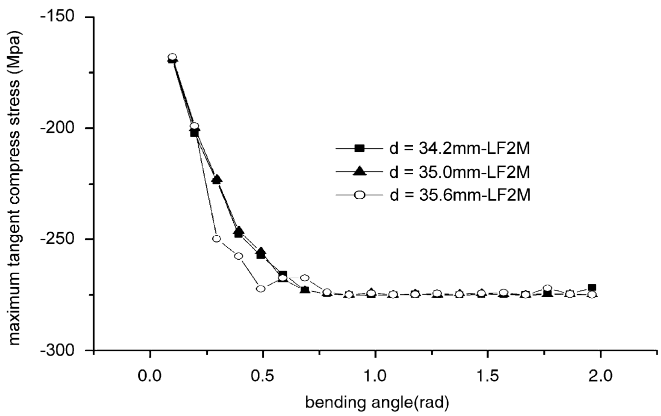

Fig. 6. Maximum tangent stress with different mandrel diameters ($e = 6$ mm, $n = 2$).

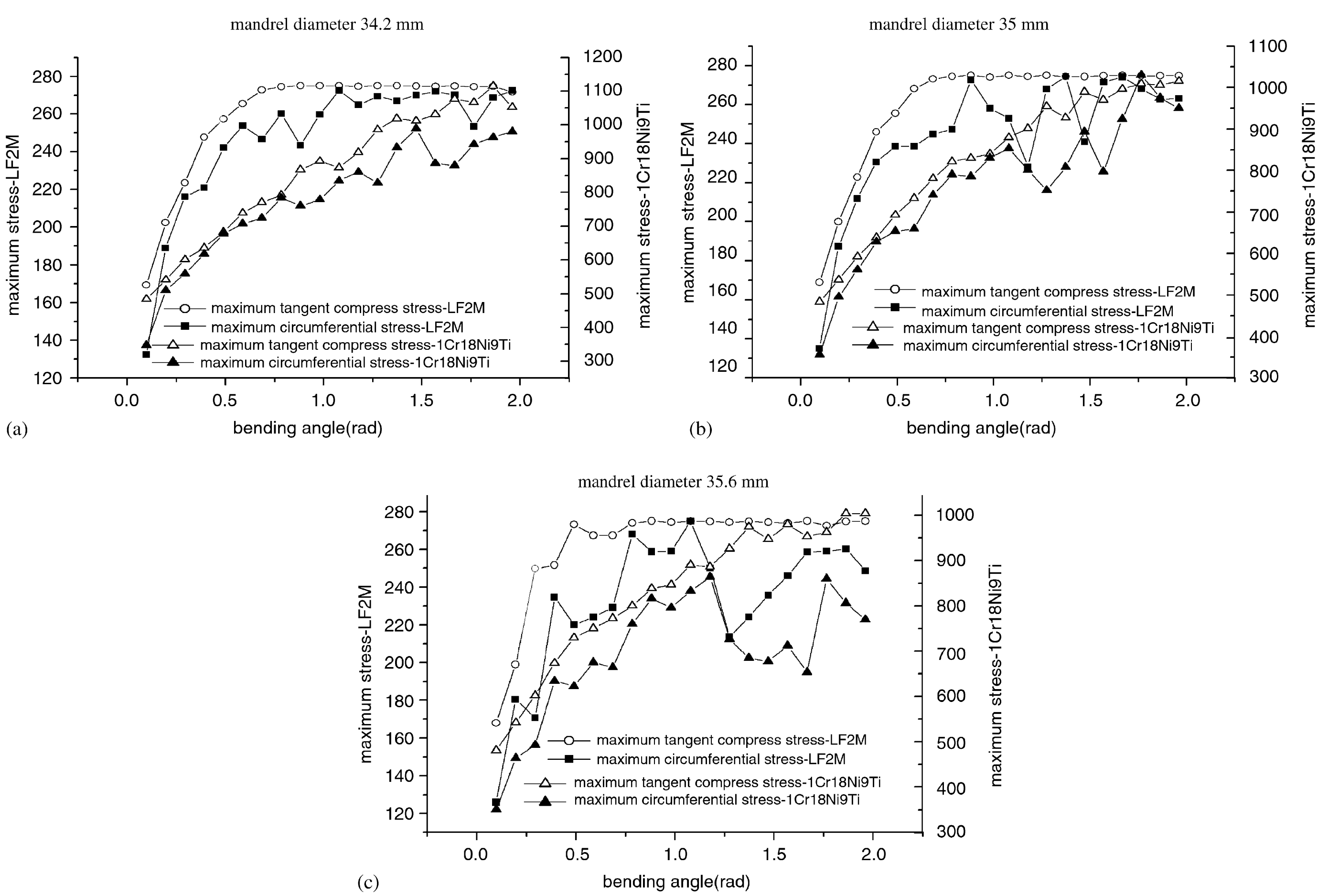

Fig. 7. History curve of maximum tangent and circumferential compressive stress with different mandrel diameters ($e = 6$ mm, $n = 2$): (a) mandrel diameter 34.2 mm; (b) mandrel diameter 35 mm; (c) mandrel diameter 35.6 mm.

4.2. Effects of mandrel extension length

The bending processes with the mandrel extension length 6, 8, 10 and 11 mm have been simulated, respectively. The mandrel diameter is 35.6 mm and the ball number is 2. In the simulation, it is found that the wrinkling instability does not occur in all cases.

The maximum tangent stress distribution for the different mandrel extension lengths has been investigated. Fig. 8 shows the history curves of the maximum tangent stress with various mandrel extension lengths.

It is found that the difference between the maximum tangent compressive stress and the tension stress turns small with the mandrel extension length rises. Even the difference becomes negative and is far less than the ones with the mandrel diameters 34.2 and 35.0 mm, when the extension length is 11 mm. As a result, although the mandrel extension length enables the neutral axis move towards outside to some extent, the significance for restraining the wrinkling is much less than mandrel diameters.

Fig. 9 reveals that the difference between the maximum tangent and the circumferential compressive stresses remains stable and thus wrinkling possibility is unchanged with the different mandrel extension lengths. That is because when the extension length is less than nose radius r, it means that the mandrel and wiper die does not cooperate well and the wrinkling is prone to occur. But as discussed in Section 2, when the extension length is larger than r, its function of restraining wrinkling is accomplished totally and the anti-wrinkling ability is limited when the mandrel extension is put forward further.

It is noted that outside tube will over thin and even crack when mandrel extension length exceeds $e_{\max}$.

4.3. Effects of ball numbers

The bending processes without balls or with 1, 2 and 3 balls have been simulated, respectively. The mandrel diameter is 35.6 mm and the mandrel extension length is 6 mm.

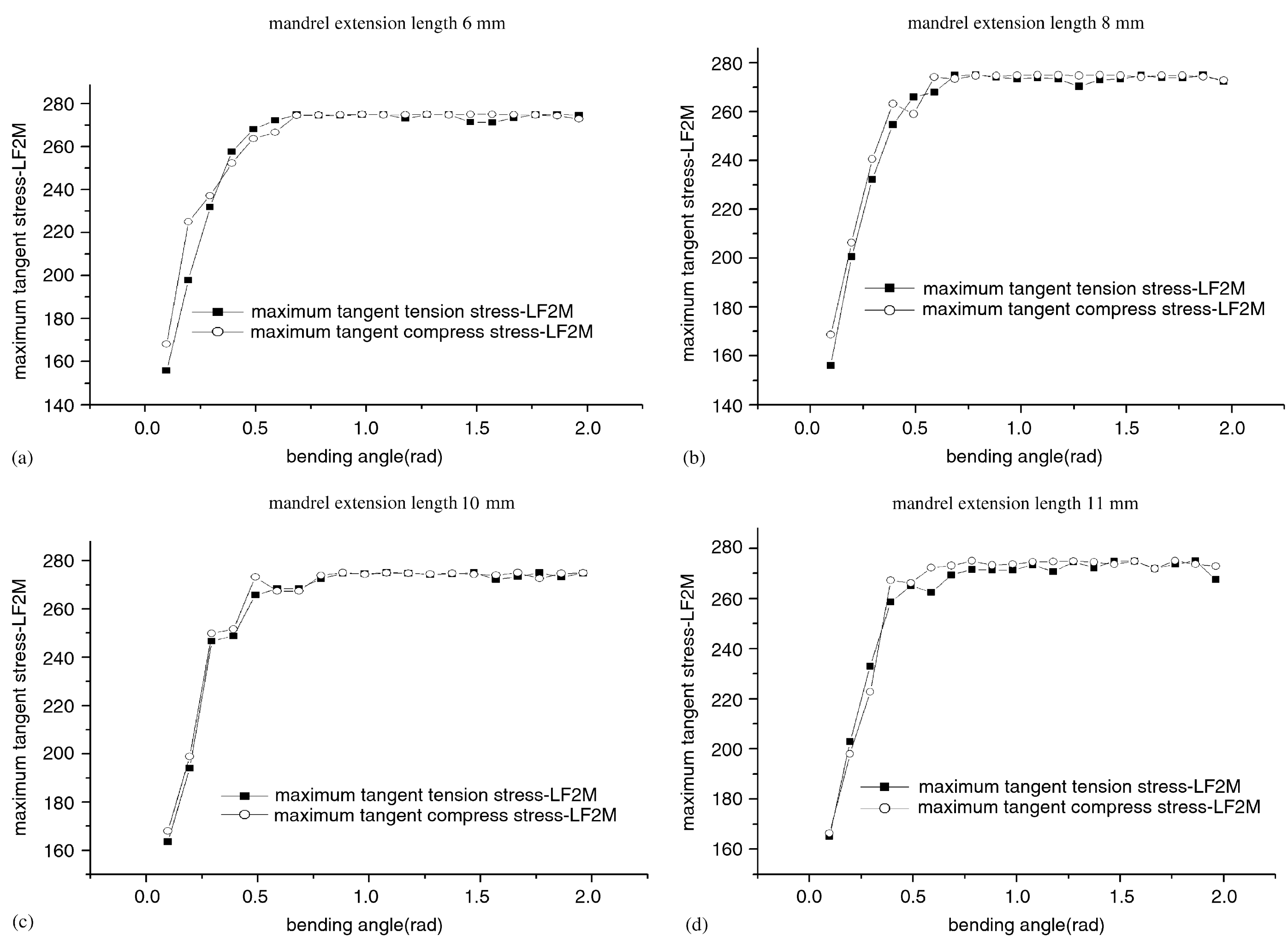

Fig. 8. History curve of maximum tangent stress with different mandrel extension length ($d = 35.6$ mm, $n = 2$): (a) mandrel extension length 6 mm; (b) mandrel extension length 8 mm; (c) mandrel extension length 10 mm; and (d) mandrel extension length 11 mm.

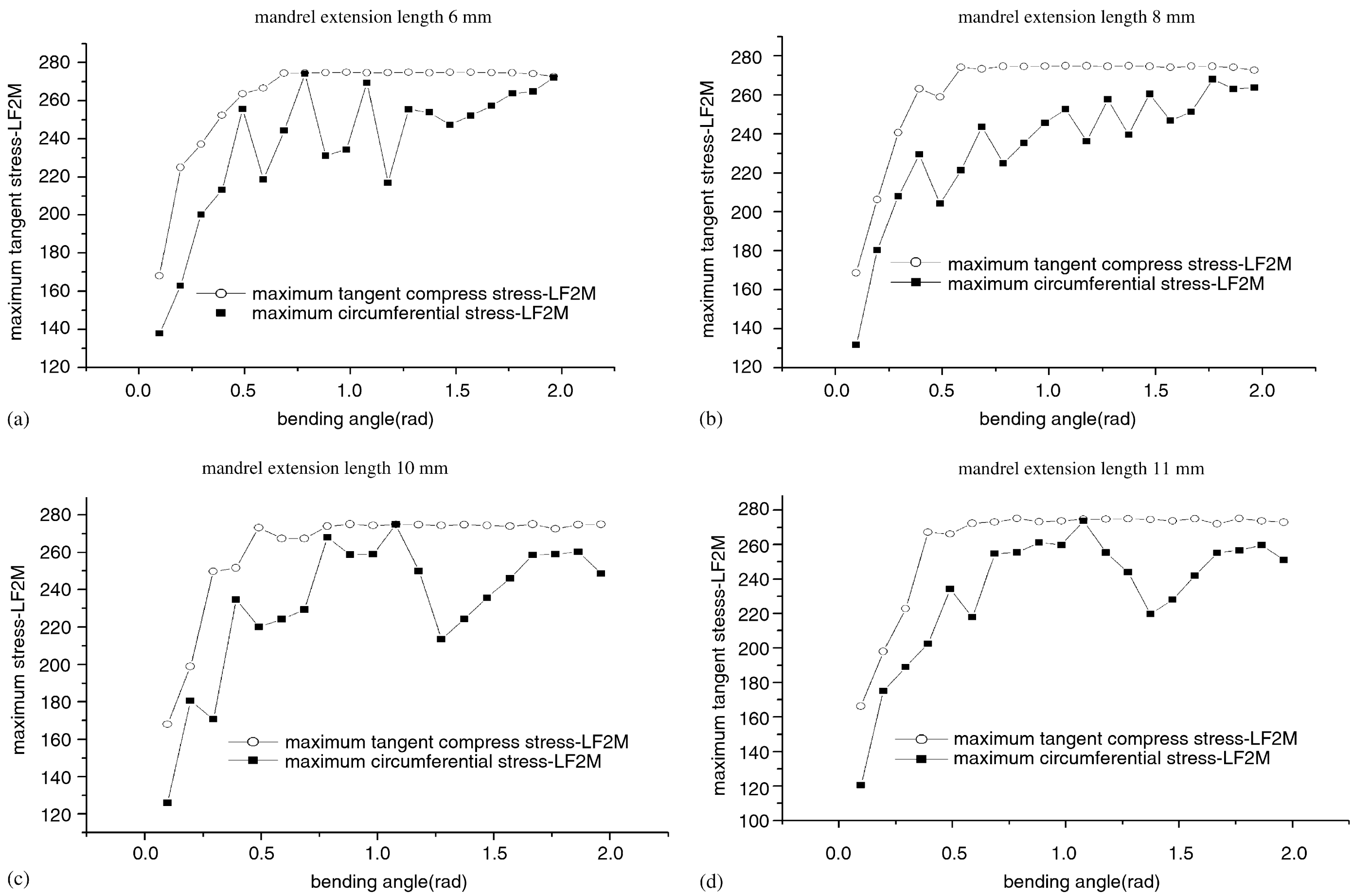

Fig. 9. History curve of maximum tangent and circumferential compressive stress with different mandrel extension length ($d = 35.6$ mm, $n = 2$): (a) mandrel extension length 6 mm; (b) mandrel extension length 8 mm; (c) mandrel extension length 10 mm; and (d) mandrel extension length 11 mm.

Fig. 10 shows the equivalent plastic strain contour with various ball numbers. It can be seen that wrinkling occurs at the front end of bent tube when the ball number is 0 or 1, while the bending processes are stable with 2 and 3 balls.

The history curves of the maximum tangent stress with various ball numbers are studied. It is found that the maximum tangent compressive stress is larger than tension stress during the stable bending process when the numbers of ball are 0 or 1, and the maximum difference is 2.1%, which is far less than the ones with the 2 and 3 balls. When the ball number is 2 and 3, there's little difference between the two conditions. As a result, balls can make the neutral axis move towards outside and improve the anti-wrinkling ability.

Fig. 11 reveals that the difference between the maximum tangent and the circumferential compressive stresses with 0 or 1 ball is less than that with 2 or 3 balls, which may result into the wrinkling instability. Namely, more balls may increase tube's anti-wrinkling ability to some extent.

From Fig. 12, it is found that mandrel balls improve the cross-section distortion degrees efficiently, while the role of the ball numbers for controlling the cross-section distortion is limited when the ball number exceeds 2. That's because for the scheduled 90° of bent tube, the cross-section with the maximum distortion degree is located at about 45°, and 2 balls may ensure balls extension end support the critical dangerous sections. By ensuring the same other forming conditions, the experiment has been carried out to verify the conclusion with 1, 2 and 3 balls, respectively. It is found that the difference between the maximum distortion degrees with 1 and 2 balls reaches 7%, while the difference with 2 and 3 balls is within 0.5%.

Furthermore, with the increasing ball numbers, the extrados thinning degree will occur and the increased backward dragging force may cause the relative slipping between the tube and the clamp die, which may cause wrinkling. Also, the more ball numbers may enlarge the connection difficulty between the balls and increases the manufacturing costs immensely. Consequently, for the bending operation with certain bending

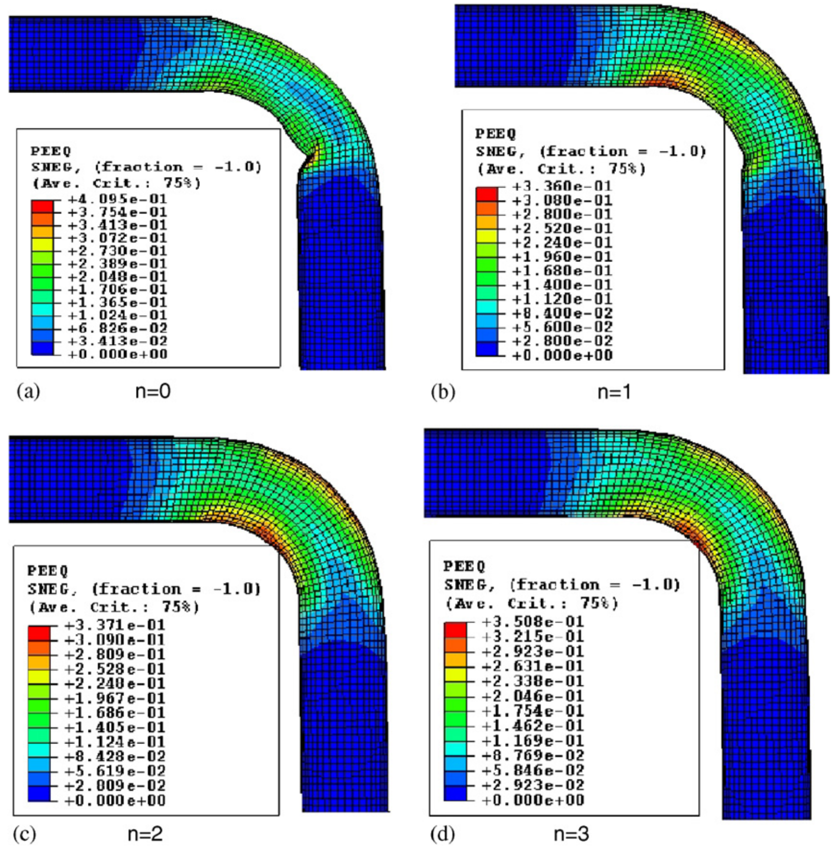

Fig. 10. The equivalent plastic strain contour with various ball numbers: (a) 0 ball; (b) 1 balls; (c) 2 balls; and (d) 3 balls.

angle, the dangerous sections may be calculated and thus ball number can be obtained by Eq. (5).

5. Conclusions

In the study, some formulas have been deduced in order to select the mandrel diameter d, the mandrel extension e, the ball numbers n, the balls thickness k, the space length between balls p and the nose radius r. And a 3D elastic–plastic FE model of the NC bending process has been established using the dynamic explicit FE code ABAQUS/Explicit. Both the analytical and FE models are validated by the experiments. Further, the role of the mandrel in the NC precision bending process such as the wrinkling prevention has been revealed. The results show the following:

(1) The wrinkling in the tube NC bending process is conditional on biaxial compressive stress state; the smaller the difference between the biaxial stresses is, the more possibility of wrinkling occurs. And the anti-wrinkling abilities of both LF2 M and 1Cr18Ni9Ti tube are the same.
(2) If the mandrel of larger sizes are used, the neutral axial will be moved outward and the difference between the in-plane compressive stresses becomes more obvious, which may increase the minimum wrinkling energy and anti-wrinkling ability, but make outside tube over-thinning.
(3) When the mandrel extension length increases, the neutral axial will be moved outward and the difference between the in-plane biaxial compressive stresses becomes larger to some extent, but the significance for restraining the wrinkles is much less than the one of the mandrel size. The excessive extension will cause the tube over-thin or even crack.
(4) The significance of ball numbers' effect on the neutral axial position and the difference between the biaxial compressive stresses is between the ones of the mandrel size and mandrel extension length. Though increasing the ball numbers improves the cross-section distortion degrees efficiently, the role for controlling the distortion is limited when the ball number exceeds the number calculated by the proposed formulas. Beside, increasing the ball numbers will enhance the over-thinning and increase manufacturing cost.

The results may help to the better understand of the mandrel's role on the improvement of forming limit and forming quality from point of plastic forming mechanism.

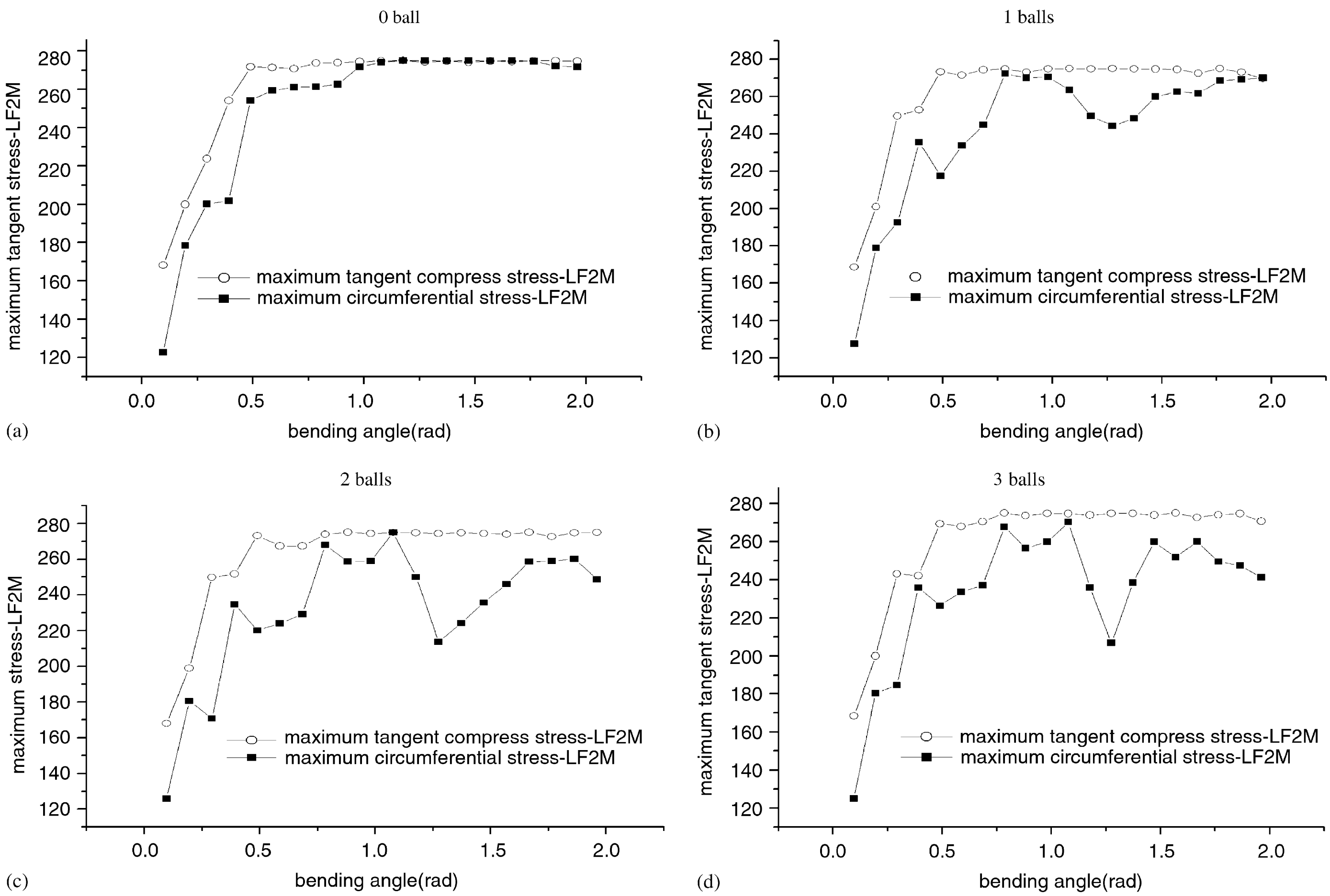

Fig. 11. History curve of maximum tangent and circumferential compressive stress with different ball numbers ($d = 35.6$ mm, $n = 2$).

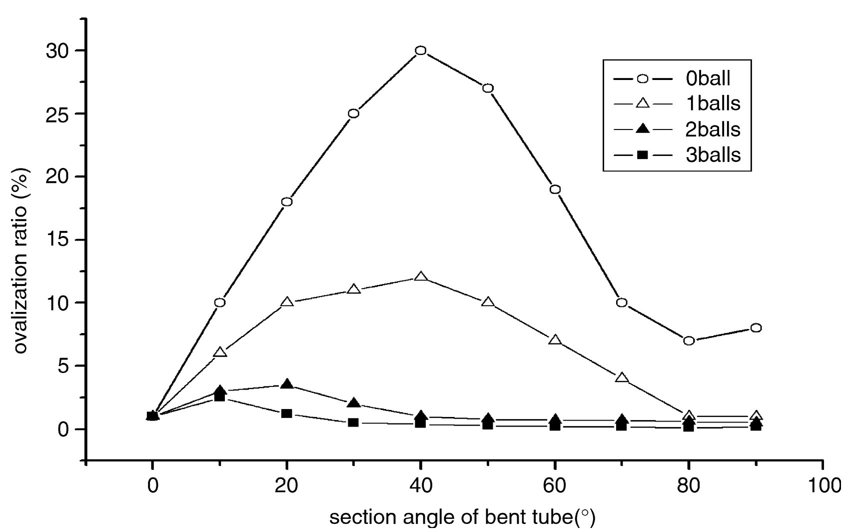

Fig. 12. Cross-section distortion degree of different sections with various ball numbers.

Acknowledgments

The authors would like to thank the National Natural Science Foundation of China (Nos. 59975076 and 50175092), the National Science Found of China for Distinguished Young Scholars (No. 50225518), the Teaching and Research Award Program for Outstanding Young Teachers in Higher Education Institutions of MOE, PRC and the Specialized Research Fund for the Doctoral Program of Higher Education of MOE, PRC

(20020699002), Aviation Science Foundation (04H53057) for the support given to this research.

References

[1] H. Yang, Z.C. Sun, Y. Lin, M.Q. Li, Advanced plastic processing technology and research progress on tube forming, Journal of Plasticity Engineering 8 (2) (2001) 86–88 (in Chinese).
[2] T. Welo, F. Paulsen, T.J. Brobak, The behaviour of thin-walled aluminium alloy profiles in rotary draw bending—a comparison between numerical and experimental results, Journal of Materials Processing Technology 45 (1994) 173–180.
[3] F. Paulsen, T. Welo, Application of numerical simulation in the bending of aluminium-alloy profiles, Journal of Materials Processing Technology 58 (1996) 274–285.
[4] Z. Hu, J.Q. Li, Computer simulation of pipe-bending processes with small bending radius using local induction heating, Journal of Materials Processing Technology 91 (1999) 75–79.
[5] Y. Jae-Bong Yang, B.-H. Jeon, S.-I. Oh, The tube bending technology of a hydroforming processes for an automotive part, Journal of Materials Processing Technology 111 (2001) 175–181.
[6] K. Trana, Finite element simulation of the tube hydroforming processes, bending, performing and hydroforming, Journal of Materials Processing Technology 127 (2002) 401–408.
[7] M. Zhan, H. Yang, Z.Q. Jiang, Z.S. Zhao, Y. Lin, A study on a 3D FE simulation method of the NC bending process of thin-walled tube, Journal of Materials Processing Technology 129 (2002) 273–276.
[8] Y. Lin, H. Yang, M. Zhan, Development of FEM simulation system for thin-walled tube NC bending process, Chinese Journal of Mechanical Engineering 39 (8) (2003) 101–105 (in Chinese).
[9] H. Li, H. Yang, M. Zhan, L.G. Guo, R.J. Gu, Wrinkling limit based on FEM virtual experiment during NC bending process of thin-walled tube, Material Science Forum 471–472 (2004) 498–502.
[10] H. Li, H. Yang, M. Zhan, L.G. Guo, R.J. Gu, Numerical research on wrinkling onset during the NC bending process of thin-walled tube, in: Proceedings of the Sixth International Conference on Frontiers of Design and Manufacturing, Xi'an, 21–23 June 2004, pp. 435–436.
[11] Hibbit Karlson and Sorensen Inc., ABAQUS Version 6.4, 2005.